

CIRP ANNALS 1989

Manufacturing Technology

BERICHTE DER INTERNATIONALEN FORSCHUNGSGEMEINSCHAFT FÜR MECHANISCHE PRODUKTIONSTECHNIK

ANNALS OF THE INTERNATIONAL INSTITUTION FOR PRODUCTION ENGINEERING RESEARCH

ANNALES DU COLLÈGE INTERNATIONAL POUR L'ÉTUDE SCIENTIFIQUE DES TECHNIQUES DE PRODUCTION MÉCANIQUE



VOLUME 38/1/1989

39. MITGLIEDERVERSAMMLUNG DES CIRP
39th GENERAL ASSEMBLY OF CIRP
39^e ASSEMBLÉE GÉNÉRALE DU CIRP

Trondheim (Norway) 21st to 26th of August, 1989

EDITORIAL COMMITTEE

Professor J. R. Crookall, Cranfield Institute of Technology (UK)
Professor H. Kudo, Yokohama National University (Japan)
Professor E. Lenz, Technion, Haifa (Israel)
Professor R. Levi, Politecnico di Torino (Italy)
Professor D. Schmoeckel, Technische Hochschule Darmstadt (West Germany)
Professor B. F. von Turkovich, University of Vermont (USA)
Professor M. Véron, Université de Nancy (France)

CIRP Secrétariat
10, rue Mansart
75009 Paris
Tél. (1) 45 26 21 80, Fax (1) 40 16 40 75

Published by 'Technische Rundschau'
A Division of Hallwag Publishers
Berne and Stuttgart
ISBN 3-905-277-11-3

© 1989 Hallwag Ltd., Berne

Printed in Switzerland

Table of Contents

Authors: (1) Active Members
(2) Corresponding Members

Session on Assembly (A)

H. Weule, T. Friedmann/W. Eversheim (1) Computer-aided product analysis in assembly-planning . . .	1
N. Roth, K.G. Günther (1), P. Rummel, W. Beutel Model generation for sensor: guided flexible assembly systems	5
T. Komatsu (2), S. Nagashima, H. Tsukada An automatic adjustment system for VCR magnetic heads on cylinder units	9
L.M. Rosario, W.A. Knight (2) Design for assembly analysis: extraction of geometric features from a CAD system data base	13
T. Arai/H. Makino (1) Analysis of part insertion with complicated shapes . . .	17
J. Milberg (1), H. Diess Assembly simulation - an efficient tool for assembly-oriented design	21
M. Shpitalni (2), G. Elber, E. Lenz (1) Automatic assembly of 3-D structures via connectivity graphs	25
H. Janocha, E. Menzel/H.K. Tönshoff (1) Assembly of PIH-devices with robots	29
H. Van Brussel (1), P. Valckenaers Hierarchical control of a generic flexible assembly cell	33
C.J.M. Heemskerck/C.A. Van Luttervelt (1) The use of heuristics in assembly sequence planning . . .	37
H.J. Warnecke (1), M.E. Domm Assembly by industrial robots with CAD/CAM and vision control periphery	41

Session on Cutting (C)

E.J.A. Armarego (1), N.P. Deshpande Computerized predictive cutting models for forces in end-milling including eccentricity effects	45
H. Schulz/G. Spur (1) Aspects on cutting mechanism in high speed cutting . . .	51
T.H.C. Childs, W.I. Mahdi/G. Barrow (1) On the stress distribution between the chip and tool during metal turning	55
M.C. Shaw (1), T.C. Ramaraj Brittle fracture of cutting tools	59
V.A. Ostafiev (1), A.N. Noshchenko Thermostrength of carbide tools	65
A. Ber (1), M. Goldblatt The influence of temperature gradient on cutting tool's life	69
C. Nedess, W. Hintze/C.A. Van Luttervelt (1) Characteristic parameters of chip control in turning operations with indexable inserts and three-dimensionally shaped chip formers	75
R. Wertheim (1), J. Rotberg, A. Ber (1) Investigation of turning systems where controlled elasticity improves machining performance	81
T. Hoshi (1), H. Zhao, T. Hosoi Study of a high performance drill geometry	87
E. Kuljanic (1) Method for increasing tool life in hobbing (MITL-hobbing)	91
K. Uehara (1), H. Takeshita Prognostication of the chipping of cutting tools	95
R. Teti/G.F. Micheletti (1) Tool wear monitoring through acoustic emission	99
B. Lindström (1) Cutting data field analysis and predictions. Part 1. Straight Taylor slopes	103

G. Lorenz (1) Principal component analysis in technology	107
M. Masuda, Y. Maeda, T. Nishiguchi, M. Sawa, R. Ito/ N. Ikawa (1) A study on diamond turning of Al-Mg alloy - Generation mechanism of surface machined with worn tool	111
T. Moriwaki (2), K. Okuda Machinability of copper in ultra-precision micro diamond cutting	115
W. König (1), P. Grass Quality definition and assessment in drilling of fibre reinforced thermostets	119
L. de Chiffre (2) Cut welding	125

Session on Design (DN)

H. Schmekel/G. Sohlenius (1) Functional models and design solutions	129
K. Ando, H. Yoshikawa (1) Generation of manufacturing information in intelligent CAD	133
K. Iwata (1), M. Onosato A computer aided conceptual design system of machine . . .	137
Y. Ito (2), H. Shinno, S. Nakanishi Designer's thinking pattern in the basic layout design procedure of machine tool - validity evaluation of thinking block	141
S.R. Kumara, I. Ham (1), M. Al-Hamando, K. Goodnow Causal reasoning and data abstraction in component design	145
F. Kimura (2), H. Suzuki A CAD system for efficient product design based on design intent	149
T. Lenau, L. Alting (1) Intelligent support systems for product design	153
G. Boothroyd (1), P. Radovanovic Estimating the cost of machined components during the conceptual design of a product	157
P. Dewhurst (2), C. Blum Supporting analyses for the economic assessment diecasting in product design	161
R.J. Menassa, W.R. de Vries (2) Locating point synthesis in fixture design	165
M.A. Arıkan, B. Kaftanoğlu (1) Dynamic load and root stress analysis of spur gears . . .	171
M. Lossie, J. Peters (1), H. Van Brussel (1) Design philosophy in filament winding	175
F. Jovane (1), L. Carlesi The elementary machine: an atomic model to analyse and devise production systems	179

Session on Physical and Chemical Machining (E)

K.P. Rajurkar, W.M. Wang/R.P. Lindsay (1) A new model reference adaptive control of EDM	183
F. Staelens, J.P. Kruth (2) A computer integrated machining strategy for planetary EDM	187
D.F. Dauw (2), H. Sthioul, R. Delpretti, C. Tricarico Wire analysis and control for precision EDM cutting . . .	191
T. Masuzawa (2), J. Tsukamoto, M. Fujino Drilling of deep microholes by EDM	195
D. Kremer, J.L. Lebrun, B. Hosari, A. Moisan (1) Effects of ultrasonic vibrations on the performances in EDM	199
M. Fukui, N. Kinoshita (1) Developing a "mole" electric discharge digging machining	203
S. Enache (1), C. Opran The mathematical model of the ECM with magnetic field	207

Y. Furukawa (1) Computer simulation of anisotropic etching process of single crystal silicon	211
F.O. Olsen/L. Alting (1) Cutting front formation in laser cutting	215
H.K. Tönshoff (1), C. Emmelmann Laser cutting of advanced ceramics	219

Session on Forming (F)

A. Gräber, K. Pöhlant/K. Lange (1) A new approach to the torsion test for determining flow curves	223
N. Becker, K. Pöhlant/K. Lange (1) Improvement of the plane-strain compression test for determining flow curves	227
A.N. Bramley, J.D. Lord/B.J. Davies (1) Determination of wear resistance of hot work die materials	231
J. Tirosh (1), D. Iddan Technological implications of high speed forming processes	235
N. Alberti (1), L. Cannizzaro, L. d'Acquisto, E. Lo Valvo, F. Micari Computer-aided simulation of die filling processes	239
B.L. Jenkins, S.I. Oh (2), T. Altan (1) Investigation of defect formation in a 3-station closed- die forging operation	243
J.S. Gunasekera (2), E.J. Chitty, V.S. Kiridena Analytical and physical modeling of the buckling behaviour of high aspect ratio billets	249
K. Shinozaki, H. Kudo (1) Further investigation of cold lateral extrusion to form staggered branches from a cylindrical billet	253
T. Ishikawa, N. Yukawa, Y. Tozawa (1) Optimization of pass schedule from the view point of shape and profile of cold rolled strip	257
R. Arrieux (2), M. Boivin Theoretical determination of the forming limit stress curve for isotropic sheet materials	261
E. Doege (1), B. Breidohr Analysis of stretch forming process - simulation and experiment	265
J.C. Gelin, J.L. Daniel/A. Moisan (1) Computer modeling of sheet metal forming by the finite element method	271
D. Schmoeckel (1), A. Skiadas, P. Mazilu Analytical description and FE simulation of the tube inverse pressing	275
A. Makinouchi, H. Ogawa/Y. Tozawa (1) Simulation of sheet bending processes by Elastic-Plastic finite element method	279
M. Kiuchi (2) CAD system for cold roll-forming	283
T. Kuwabara, T. Jimma, I. Matsuoka/H. Kudo (1) Deep drawing of shells having slopes in the base	287
A. Raggenbass, J.S. Reissner (1) Stamping - laser combination in sheet processing	291
L.G. Cser/J. Prohaska (1) CAD/CAM integration of prefabrication and prefab design	295
A.G. Mamalis (1), G.N. Gioftsidis, A. Szalay, O. Boday The shock wave compaction of high temperature super- conducting powders into cylindrical components	297

D.R. Allanson, S. Kelly, S. Terry, J.L. Moruzzi, W.B. Rowe (1) Coping with compliance in the control of grinding processes	311
I. Inasaki (2) Dressing of resinoid bonded diamond grinding wheels	315
R. Porat (2), Y. Yarnitsky The effect of diamond powder grain size on the rate of polishing diamond crystallographic planes	319
T. Matsuo (2), S. Toyoura, E. Oshima, Y. Ohbuchi Effect of grain shape on cutting force in superabrasive single-grit tests	323
T. Nakano, K. Abe, H. Kubo/A. Kobayashi (1) Newly developed dressing technology for cutting-off sialon (Si-AI-O-N) ceramics	327
Y. Namba, R. Wada, K. Unno, A. Tsuboi/K. Okamura (1) Ultra-precision surface grinder having a glass-ceramic spindle of zero-thermal expansion	331
H.W. Zheng (1), G.G. Cai, S.L. Wang, S.X. Yuan An experimental study on mechanism of cermet grinding	335

Session on Machine Tools (M)

P. Boucher, D. Dumur, Z. Kapusta/P.J. Duchaine (1) Improvement of productivity with predictive control in speed and position	339
Y. Hatamura, T. Nagao, M. Mitsuishi, H. Tanaka/ K. Iwata (1) Development of a force controlled automatic grinding system for actual NC machining centers	343
M.A. Mannan, S. Broms/B. Lindström (1) Monitoring and adaptive control of cutting process by means of motor power and current measurements	347
M. Szafarczyk (1), B. Klein, W. Szala Extension of typical CNC systems by external controllers	351
F. de Schepper, K. Yamazaki, T. Shigemura, M. Inai/ T. Hoshi (1) Development of an ASIC performing high speed current loop processing of servo motor control for mechatronics applications	355
P.C. Mulders (2), J. Jansen, J.M.L. Pijls Optimal trajectory control of a linear robotarm by a state space method	359
K. Wang, O. BJORKE (1) An efficient inverse kinematic solution with a closed form for five-degree-of-freedom robot manipulators with a non-spherical wrist	365
G. Duellen (1), H.D. Stahlmann, X. Liu An off-line planning and simulation system for the programming of coating robots	369
R. Stadelmann/P.E. Gygax (1) Computation of nominal path values to generate various special curves for machine tools	373
E.I. Rivin, H.L. Kang/L. Kops (1) Improving dynamic performance of cantilever boring bars	377
M. Weck (1), J. Alldieck The originating mechanisms of wheel regenerative grinding vibrations	381
M. Rahman (2) A study on the deviation of shape of a turned workpiece clamped by multiple jaws	385
M. Zatarain/F. Le Maitre (1) Behaviour of covering materials for guideways	389
H. Hädeby/G. Sohlenius (1) Increasing availability and efficiency by monitoring the cutting process in a lathe during production with limited manpower	393

Session on Abrasive Process (G)

E. Saljé (1), W. Hörsemann, M. Klyk Grinding of cylindrical blanks with controlled workspeed	303
R.J. Baylis, B.J. Stone (1) The effect of grinding wheel flexibility on chatter	307

Session on Optimization (O)

J.R. Boerma, H.J.J. Kals (1) Fixture design with FIXES: the automatic selection of positioning, clamping and support features for prismatic parts	399
J.K. Li, C. Zhang/Y.Z. Zhang (1) Operational dimensions and tolerances calculation in CAPP systems for precision manufacturing	403
J. Peklenik (1), A. Sluga Contribution to development of a generative CAPP system based on manufacturing process topology	407
E. Ramsli/F.O. Rasch (1) Modelling and simulation of manufacturing systems	413
S. Takata (2), M.D. Tsai, M. Inui, T. Sata (1) A cutting simulation system for machinability evaluation using a workpiece model	417
W. Massberg/M. Weck (1) Problemneutrales Verfahren zur Simulation, Steuerung und Diagnose von Productionanlagen	421
G. Chryssolouris (2), M. Domroese An experimental study of strategies for integrating sensor information in machining	425
Y. Takeuchi, M. Sakamoto, Y. Abe, R. Orita/T. Sata (1) Development of a personal CAD/CAM system for mold manufacture based on solid modeling techniques	429
R.T. Yap/V.C. Venkatesh (1) On the formulation of numerical control algorithms using computational geometry	433
F.L. Krause, H. Jansen, G. Grossmann/G. Spur (1) Automatic scanning and interpretation of engineering drawings for CAD processes	437
W. Eversheim (1), H. Rozenfeld, G. Marcziński Requirements on interfaces and data models for NC-data transfer in view of computer integrated manufacturing	443
A. Novak, G. Ossbahr, F. Wikström/N. Mårtensson (1) A digital link for adaptive control and on-line FMS- applications	447
B. Mutel, R. De Guio/A. Clément (1) Recognition of cellular manufacturing under management constraints	451
S.C.Y. Lu/I. Ham (1) Machine learning techniques for group technology applications	455
R.R. Slatter, T.M. Husband (1), C.B. Besant, M.R. Ristic A human-centred approach to the design of advanced manufacturing systems	461
J.S. Edghill, D.R. Towill/T.M. Husband (1) Dynamic behaviour of fundamental manufacturing system design strategies	465
G. Pritschow (1), M. Jantzer Free-ranging vehicles with minimal space expense as high flexible transport systems	469
S.D. Sun, J.Y. Zhu (1) Variable structure model reference adaptive control system with application in robots	475
F. Giusti (1), M. Santochi (2), G. Dini KAPLAN: a knowledge-based approach to process planning of rotational parts	481
K.I. Lee, J.W. Lee, J.M. Lee (2) Pattern recognition and process planning of prismatic workpieces by knowledge based approach	485
V. Majstorović, V. Milacic (1) An expert system for diagnosis and maintenance in FMS	489
S. Kanai, M. Sugawara, K. Saito/K. Okamura (1) The development of the intelligent machining cell	493
A. Villa (2) Knowledge engineering rules for manufacturing system design (KERMAS): specify and justify FMS incremental implementations	497

Session on Dimensional Metrology in Quality Assurance (Q)

D.C. Thompson/P.A. McKeown (1) The design of an ultra-precision CNC measuring machine	501
J.W.M.C. Teeuwse, J.A. Soons, P.H.J. Schellekens (2)/ A.C.H. Van der Wolf (1) A general method for error description of CMMs using polynomial fitting procedures	505
L. Nawara (1), M. Kowalski, J. Sladek The influence of kinematic errors on the profile shapes by means of CMM	511
H. Aoyama, M. Kawai, T. Kishinami/N. Taniguchi (1) A new method for detecting the contact point between a touch probe and a surface	517
G.N. Peggs/P.A. McKeown (1) Creating a standards infrastructure for co-ordinate measurement technology in the UK	521
G.X. Zhang (1) A study on the Abbe principle and Abbe error	525
W.J. Wills-Moreen (2), T. Wilson The design and manufacture of a large CNC grinding machine for off-axis mirror segments	529
S.M. Wu (2), V. Ni Precision machining without precise machinery	533
B.H. Zhuang, C.S. Ih, L.Q. Xiang, C.W. Yang, K.Q. Lu, Y. Shen, R.S. Tian/G.X. Zhang (1) Using compensated HOE in optical head	537
Y. Yamauchi, G.I. Yasuda, K. Tachibana/H. Yoshikawa (1) In-process measurement system for radiation spectrum in laser welding	541

Session on Surfaces (S)

K.J. Stout, P.J. Sullivan/W.B. Rowe (1) The analysis of the three dimensional topography of the grinding process	545
T. Semba, K. Sakuma, Y. Tani, H. Sato (1) Thickness measurement of metallurgically damaged layer on a ground surface using an acoustic microscope	549
Z.J. Yuan, Z.G. Hu/A. Kobayashi (1) Surface integrity of grinding of bearing steel GCr15 with CBN wheels	553
A.S. Lavine, S. Malkin (1), T.C. Jen Thermal aspects of grinding with CBN wheels	557
P. Stepien/M. Szafarczyk (1) Generation of regular patterns on ground surfaces	561
J.H. Dautzenberg (2), J.A.B. Van Dijck, J.A.G. Kals (1) Metal structures by friction in mechanical working processes	567
P.M. Leonardo (2), A.A.G. Bruzzone Influence of surface roughness parameters on the mechanical strength in metal gluing	571

Thermostrength of Carbide Tools

V. A. Ostafiev (1), A. N. Noshchenko — Kiev Polytechnic Institute
Received on January 13, 1989

ABSTRACT:

The tool volume thermal-stressed state has been investigated. Due attention is paid to estimating the role of thermal and mechanical loads and adequately selecting the criteria of sizing-up the tool's strength. The data obtained as a result of the performed investigations are used so as to explain the experimentally established characteristics of the tool's wear and fracturing in the process of continuous and interrupted machining.

KEY WORDS:

Tool, strength, FEM.

I. Introduction

In the process of machining, the cutting tool takes up considerable thermal and mechanical loads. The investigation of temperature and/or stress distribution in the tool's cutting area is, therefore, an important issue both for the theory and practice of machining.

There are quite a few studies dealing with the temperature variation in machining, as well as those tackling the temperature-wear problems. As for the tool's strength, it was paid attention to by fewer authors. It is attributable, on the one hand, to the lack of reliable experimental methods of determining the stressed state under conditions of a more significant dynamic pattern of thermal and mechanical loads, particularly, during the interrupted cutting, and on the other hand, to the sophisticated nature of the theoretical study of stresses in the cutting tool.

Analysis of the available literature [1,2,3,4,9] indicates that the majority of strength studies ignore the combined influence of the thermal and mechanical loads, as well as the three-dimensional nature of the tool's stressed state. The strength analysis in these studies was based on comparing the stress tensor elements and the principal stresses with the strength characteristics of the instrumental material. Such an approach is far from being correct for the tool in the complex stressed state.

Invalid assumptions adopted for calculating strength parameters produced the results that did not match the experimental data and precluded the derivation of relationships demonstrating the interaction between the stressed state and the fracturing or the wear of the tool. Similar discrepancies between the theory and practice gave rise to a number of hypotheses and assumptions concerning the causes of the tool's failure.

The present paper is concerned largely with the analysis of the three-dimensional distribution of temperature and stresses inside the tool. Due attention is paid to estimating the role of thermal and mechanical loads and adequately selecting the criteria of sizing-up the tool's strength.

The data obtained as a result of the performed investigations are used so as to explain the experimentally established characteristics of the tool's wear and fracturing in the process of continuous and interrupted machining.

It should be noted that in this paper by the thermally stressed state we denote the state resulting

both from the thermal load and the mechanical loads, if any.

2. Investigation method

The heat exchange parameters and the high-temperature strength of cutting tools in a three-dimensional formulation can be calculated only using the numerical methods.

The procedure of determining the three-dimensional transient temperature fields in the cutting zone based on the finite element method has been presented by the authors in [5].

The features of the above procedure that permitted the solution of the three-dimensional problem for the transient temperature field and the heat exchange in the cutting of metals can be listed as follows: automatic generation of all initial data on the mechanic parameters of cutting, as well as the data used for finite element calculations; automatic print-out of all calculated distributions of temperature in the cross(nodal) planes and on the face with the complete or the partial data visualization; employment of explicit schemes of the temporal integration with the diagonal matrix of the heat capacity; characterization of the chip's movement and the movement of the material being machined according to the combined Euler-Lagrange procedure. The above characteristics, that the authors deem worthy of note, made it possible to reduce the time for data preparation, calculation and the analysis of the obtained results by several orders of magnitude.

The three-dimensional stressed state of the tool's cutting area was determined using the finite element method in the form of the displacement method. The tool's cutting area was digitized by means of the tetrahedral elements. High temperature gradients in the tool's contact layers necessitate the use of a dense non-uniform net of finite elements. The number of nodes for the standard conditions of calculating the strength was equal to 1000-2500. For a three-dimensional problem this led to a set of 3000 to 7500 linear algebraic equations. In addition, the allowance for the influence of the thermal load produces the appreciable non-uniformity of vector elements in the right-hand side of the equation. Solution of these simultaneous equations is fairly difficult. As far as the accuracy and computation time were concerned, excellent results were obtained using the variation-gradient method [7] of solving the simultaneous linear algebraic equations.

The tool's cutting area strength was estimated

considering the distribution of principal stresses $\sigma_1, \sigma_2, \sigma_3$, the stress intensity σ_1 and the equivalent stress σ_e , which is determined by the following relationship [1]:

$$\sigma_e = \sqrt{\frac{1}{3}(\sigma_1^2 + \sigma_2^2 + \sigma_3^2)} \quad (1)$$

The parameter $\gamma = \frac{\sigma_e}{\sigma_s}$ determines the fraction of the shear strain in fracturing, σ_s is the ultimate compression strength, σ_t is the ultimate tensile strength, while A characterizes the static factor of the development of fracturing and is equal to 0.8 for the alloys of the WC-Co group or 0.7 for the alloys of the WC-TiC-Co group. Fracturing is believed to occur if $\sigma_e > \sigma_s$. The safety assurance factor in the present investigations was found from the relation $K = \frac{\sigma_s}{\sigma_e}$.

The obtained data on the empirical values of cutting forces, contact surfaces, chip ratio combined with the calculated distributions of contact loads [8], cutting thermal parameters, cutting tool geometry, thermal and physical and physico-mechanical properties of the tool material and the material being machined, were used as a source information for the finite element analysis of the three-dimensional distribution of transient temperature and stresses in the instrument's cutting area.

3. Analysis of the Results

The conducted cutting experiments and the numerical experiments lead us to believe that there exists an acceptable correlation between the stressed states of the tool's cutting area and the zones of fracturing and cutting. Of particular importance is the fact that when determining the stressed state it is necessary to take into account the combined action of mechanical and thermal loads. Ignoring the thermal factor while calculating the tool's strength parameters produces the results that do not fit the fracturing zones of contact surfaces observed during the experiment. Thus, Fig. 1, a presents the distribution of temperature in the central section of the cutting zone at the moment of its actual stabilization in the tool's cutting area. The zone of the maximum temperature values of 990 °C is located in the beginning of the second half of the contact area and it is very depth-localised.

Fig. 1, b, c, and d show the distributions of stress in the central section respectively for the cases of exclusively mechanical, thermal and combined loading of the tool's cutting area. The mechanical stress creates a stress field, whose peak equals 1140 MPa, on the rear surface below the cutting edge. The temperature gradients produce two zones of stress localization (1) a zone in the vicinity of the cutting edge ($\sigma_2 = 660$ MPa) due to the flow of the heated metal, and (2) a zone below the frontal surface in the second half of the contact with the chip ($\sigma_2 = 320$ MPa).

Dominating in the case study were the mechanical stresses. Their distribution, however, does not fit the zones of fracturing or wear either in form, or in dimensions. If allowance is made for the combined action of thermal and mechanical loads in the calculations undertaken, then there occurs the variation of both the values and the character of stress distributions.

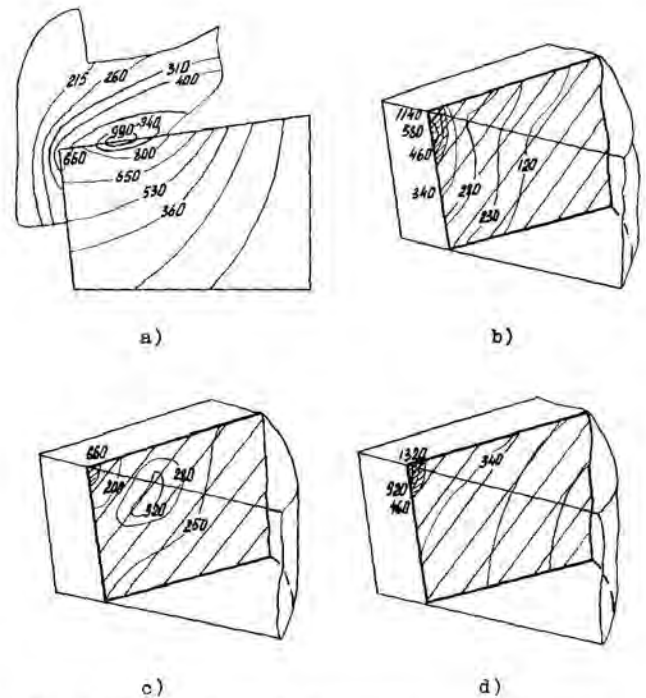


Fig. 1. Distribution of temperature and stresses in the turning of steel 40X by the tool made of alloy T15K6 ($V = 200$ m/min, $S = 0.1$ rev, $t = 0.5$ mm, $\alpha = -8^\circ$, $\gamma = 6^\circ$, $\varphi = 53^\circ$, $\varphi_1 = 14^\circ$):
a) - temperature in the central section;
b) - σ_1 as a function of mechanical load;
c) - σ_2 as a function of thermal load;
d) - σ_2 as a function of a combination of mechanical and thermal loads.

The largest values of σ_2 are related to the cutting edge and the region with the stresses $\sigma_2 > \sigma_s$ ($\sigma_s = 450$ MPa) protracts along the rear surface reaching the frontal surface, the phenomenon unobserved in the case of mechanical stresses. The extent of this region along the rear surface of the zone with a safety assurance factor below 1 was equal to 0.17 mm, while the measured wear of the rear surface was 0.16 mm. The high value of $\sigma_1 = 5910$ MPa in this zone is a special indicator of the predominantly ductile fracturing going on in this zone.

The available results testify to the fact that the distribution of stresses σ_2 gives the best correlation with the fracturing zones of contact surfaces, whereas the remaining stress invariants can be used in analysing the fracturing mode.

Fig. 2 shows the temperature field in the cutting zone along with the distribution σ_2 in the tool's cutting area when the cutting speed is brought down to 124 m/min (other machining conditions are indicated in Fig. 1). The reduction of cutting speed resulted in the chip ratio by 15%, while the contact length and the cutting force components were reduced respectively by 25 and 10%. When the cutting speed is decreased from 200 to 124 m/min, the maximum temperature values fall from 990 to 797 °C. The distribution σ_2 remained the same, while the maximum values of σ_2 decreased from 1320 to 920 MPa. The most overloaded tool parts are as usual the vicinity of the cutting edge and the rear surface, but the reduction of stresses diminishes in a fairly appreciable way the probability of the coloration and the wear rate. This regularity is confirmed by the experimental results.

The study was also investigating the thermally stressed state of the tool made of the alloy BK8 in the machining of stainless steel IX18H9T and the titanium alloy BTI-0.

The distribution of temperature and stresses σ_2 in the machining of steel IX18H9T is shown in Fig.3. This example is a convincing illustration of the thermal load's contribution. The distribution σ_2 calculated considering just the mechanical load, does not coincide with the fracturing zone of a single-point tool on the rear surface and does not suggest a possibility of the appearance of a wear crater on the frontal surface, which was, none the less, detected during the experiment. The maximum values of σ_2 related to mechanical loads were localized in the narrow layer on the frontal surface and their values ($\sigma_2 = 470$ MPa with $\sigma_b = 800$ MPa for BK8) should not be alarming. If considered in the experiment is the combined action of mechanical and thermal loads, then there occurs the variation of both the values and the character of stress distribution σ_2 .

According to the analysis data, there form two zones of fracturing on the tool's cutting planes: one on the rear surface, and the other on the frontal surface, which yields a good agreement with the experimental data. In this case the maximum values of σ_2 increase 2.5-fold reaching 1230 MPa and they are 1.5 times the ultimate strength σ_b of the alloy BK8. The highest values of the stress intensity pertain to the cutting edge equalling 2890 MPa, this fact testifying to the plastic character of edge fracturing. In the crater's thin surface layer the stress intensity σ_1 is equal to 2310 MPa, exceeding

the yield limit, as well. However, it is highly probable that the fracturing character on this site is determined by the principal stress σ_1 reaching 1200 MPa. With such values of σ_1 the brittle fracturing becomes possible.

Temperature and stress distributions σ_2 in the tool made of alloy BK8 while machining the titanium alloy BTI-0 are shown in Fig.4. In machining the titanium, plastic fracturing of the cutting edge and the rear plane is the main cause of the tool's failure. This conclusion is supported by the results of the calculations performed. The most stressed parts of the tool are the cutting edge and the rear surface. The stresses here reach 996 MPa and are in excess of σ_b . High values of $\sigma_1 = 3240$ MPa indicate the plastic character of the tool's destruction.

This computation technique was also employed for analysing the fracturing processes when the tool is used for the interrupted machining with the cooling aqueous liquid. Considering the great difficulty of obtaining all data, necessary for calculating the fracturing parameters under the real conditions of intermittent machining, the tool's heating was simulated based on the data of continuous cutting of the steel 40X using the tool made of the alloy T15K6 with the cutting speed of 200 m/min. These data were presented above. If the mechanical conditions are assumed constant, the variation of the stressed state will be determined by the transient temperature. With this assumption in mind, the study was focused on investigating stresses in the tool's cutting area during the cutting-in and quitting the machining zone (the moment of mechanical stress relaxation), as well as the stresses occurring when the tool is cooled with the different time intervals.

While the tool's cutting area cuts into the machined surface, the sudden heating of the contact surfaces causes a very unfavourable set of mechanical and thermal stresses in the vicinity of the cutting edge (see Fig.5). After 2 ms the maximum values of σ_2 become equal to 1700 MPa, while at an almost steady-state temperature they reach 1320 MPa after a passage of 40 ms. When the tool's cutting area leaves the machining zone there occurs the restructuring of the stressed state in accordance with the temperature distribution at the moment of stress relaxation. Under the contact site, there forms a centre of stresses, whose value $\sigma_2 = 465$ MPa exceeds the boundary strength σ_b for the alloy T15K6, while the stresses on the peak abruptly fall to 116 MPa. Fig.5 presents the dynamic pattern of the variation of the variation of stresses σ_2 as a result of cooling. 0.34 ms after the beginning of the cooling the maximum values of temperature drop to 751°C (the decrease is 240°C), whereas the stresses σ_2 drop to 309 MPa. After a passage of 0.68 s, the maximum values of the temperature are equal to 643°C, and the stresses σ_2 amount to 274°C, although in this case there exists the variation of the character of distribution of these parameters. The area of the maximum values of σ_2 has migrated to the end of the contact site and reached the frontal surface. In 2.04 s the temperature drops to 437°C, and the stress to 182 MPa. The maximum stresses in these localization zones occur in the rear auxiliary plane subject to active cooling. When the instrument reaches the depth of 0.295 in-

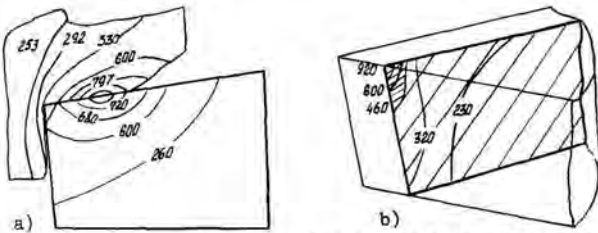


Fig. 2. Temperature (a) and stresses σ_2 (b) in the turning of steel 40X by the tool made of alloy T15K6 ($V = 124$ m/min, other parameters same as those shown in Fig. 1).

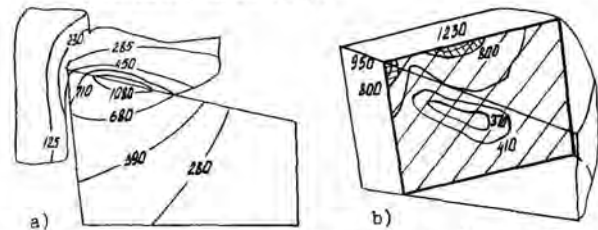


Fig. 3. Temperature (a) and stresses σ_2 (b) in the turning of the steel IX18H9T using a tool made of the alloy BK8 ($V = 60$ m/min; $S = 0.44$ mm/rev, $t = 2.8$ mm, $\alpha = 15^\circ$, $\gamma = 7^\circ$, $\varphi = 45^\circ$, $\lambda = 0^\circ$).

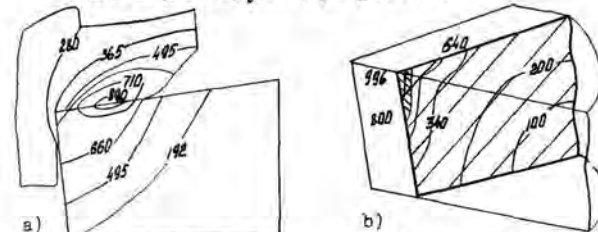


Fig. 4. The field of temperature (a) and stresses σ_2 (b) in the turning of the titanium alloy BTI-0 using the tool made of the alloy BK8 ($V = 73$ m/min; $S = 0.15$ mm/rev, $t = 0.5$ mm, $\alpha = -6^\circ$, $\varphi = 58^\circ$, $\varphi_r = 14^\circ$, $\lambda = 0^\circ$).

side the material machined, the stresses decrease to 128 MPa. From the viewpoint of statistic strength, such stress values should pose no danger. However, under conditions of the cyclic loading similar stresses may cause thermal cracks.

The investigations performed show that the dynamic pattern of the temperature variation exerts pronounced influence on the formation of the tool's stressed state. Very high heating rate (10^5 to 10^6 deg/s) of the contact surfaces when the tool penetrates the blank leads to the deterioration of strength pattern in the vicinity of the cutting edge. The deterioration in question manifests itself differently on the blank of a high alloy tool. For instance, when machining the steel 40X by the tool made of the alloy T15K6, in the initial period of cutting-in one can observe the increase of the stress level σ_2 by 30-40% compared to the period in which the tool's cutting area temperature had virtually stabilized. Equilibration of temperature is accompanied by the decrease of the values of σ_1 , σ_2 , σ_3 by one third and the increase of the σ_4 level by 30%. Under comparable conditions of machining using the BK8 tool no higher level of stresses σ_2 in the initial cutting stage has been detected. However, the dimensions of a zone with a safety assurance factor below unity are almost twice those of a similar zone existing under the steady-state temperature. The safety assurance factor in the vicinity of the T15K6 tool's top amounted to 0.25, while the similar index for the BK8 tool was equal to 0.4. These results are in agreement with a greater wear resistance of the tool made of BK8 operated during the heavy-duty interrupted machining under con-

ditions of the variable thermal and mechanical loading. Considering the fact that forces grow to their rated values in a much quicker way than does the temperature equilibration in the cutting part, one can infer that the dynamic pattern of the tool's stressed state variation in penetrating the blank controls, to a great extent, the temperature distribution character. The resulting stress level jeopardizes strength and produces fracturing or paves the way for the subsequent fracturing and/or wear. The further period of the tool's operation is characterized by the accelerated growth of the contact's length on the frontal surface as compared to the cutting forces. This alleviates the specific contact loads, and, therefore, reduces the temperature of the cutting lip. Making allowance for the thermal stress in design calculations of the tool's strength in this stage of its operation increases the general level of stresses, whose distribution is in good agreement with the zones of fracturing and wear.

When the instrument leaves the machining zone and upon the relaxation of stress load, the stress field σ_1 in the tool is formed entirely by the temperature gradients. These stresses are continuously decreased in the process of cooling and their magnitude is much lower than that characteristic of stresses during the cutting-in and the continuous cutting. However, for the alloy T15K6, whose thermal conductivity and the values of σ_D are two times those for an alloy BK8, stresses can achieve critical levels. In this case the region of maximum values of stress is located below the frontal surface in the contact zone adjacent to the rear auxiliary surface (Fig. 5). The presented analysis of the tool's operation, based on the investigation of its strength parameters, is by no means complete. The multiplicity of processes underlying the wear and fracturing of the tool prevents the formulation of a tractable theory. However, the satisfactory agreement between the three-dimensional thermally stressed state of the tool and the experimentally observed fracturing and wear of contact surfaces testifies to the particular importance of all thermal stress problems to be elucidated when designing machine tools and selecting the optimized operating conditions.

REFERENCES

- (1) Ostafiev V.A., 1979, Raschet dinamicheskoi prochnosti rezhuschego instrumenta, Mashinostroenie, Moscow.
- (2) Bhatia S.M., Pandey P.C., Shan M.S., 1980, The Thermal Condition of the Tool Cutting Edge Intermittent Cutting, "Wear", 61, No 1.
- (3) Takagi T., Shaw M., 1981, Evaluation of Fracture Strength of Brittle Tools, Annals of the CIRP, vol. 30/1:53-57.
- (4) Uehara K., Kanda Y., 1981, Fundamental Approach to the Thermal Crack of Cermet Cutting Tools, Annals of the CIRP, vol. 30/1:47-51.
- (5) Ostafiev V.A., Noshchenko A.N., 1985, Numerical Analysis of Three-Dimensional Heat Exchange in Oblique Cutting, Annals of the CIRP, vol. 34/1:137-140.
- (6) Orady P., Tlusty T., 1981, Effect of Thermal Cycling on Tool Wear in Milling, SME Manuf. Eng. Trans. vol. 9, 9th NAMRAC Proc., Dearborn, Mich.: 250-255.
- (7) Louchka A. Yu., Noshchenko O.E., Toukalevskaya N.I., 1984, Variatsionno-gradientni method, Zhurnal vychislitelnoi matematiki i matematicheskoi fiziki, t. 24, No 7:963-971.
- (8) Zorev N.N., Ostafiev V.A., 1977, Contact Loads of Cutting Tool, Transactions of 3rd International Conf. Prec. Eng. Kyoto.
- (9) Tonshoff H.K., Brinksmeier E., Bartsch S., 1987, Notch Wear and Chemically Induced Wear in Cutting with Al₂O₃-Tools, Annals of the CIRP, vol. 35/2 537-542.

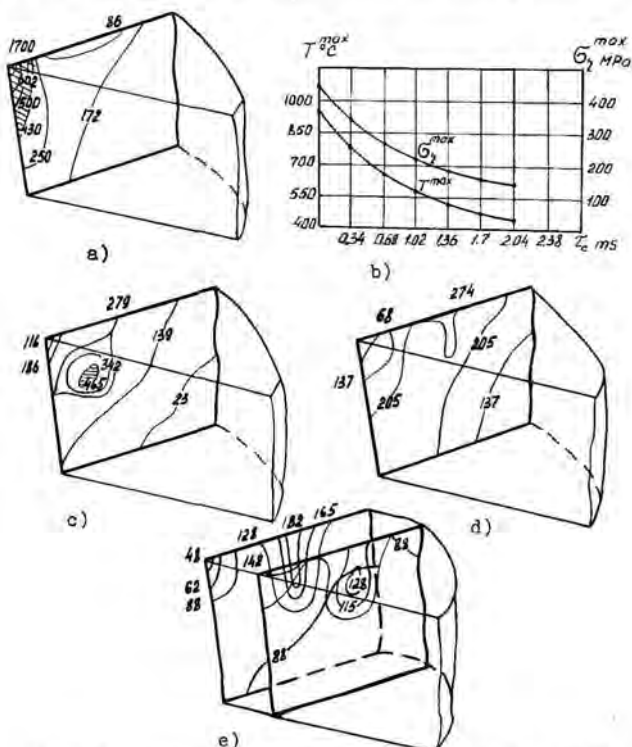


Fig. 5. Temperature and stresses σ_1 during the tool's penetration of the material, leaving the material and cooling (machining parameters are listed in Fig. 1):
 a) - stresses σ_1 , 2 ms after the penetration;
 b) - variation of the maximum values of temperature and stresses σ_1 during the tool's cooling;
 c) - stresses σ_1 at the moment of relaxation of the mechanical load;
 d) - stresses σ_1 in the cooling during 0.68 ms;
 e) - stresses σ_1 in the cooling during 2.04 ms.